JTTEE5 15:340-347
DOI: 10.1361/105996306X124329
1059-9630/$19.00 © ASM International

Peer Reviewed

Down-Selection and Optimization of Thermal-Sprayed Coatings for Aluminum Mould Tool Protection and Upgrade

Gregory John Gibbons and Robert George Hansell

(Submitted September 23, 2005; in revised form December 20, 2005)

This article details the down-selection procedure for thermally sprayed coatings for aluminum injection mould tooling. A down-selection metric was used to rank a wide range of coatings. A range of high-velocity oxyfuel (HVOF) and atmospheric plasma spray (APS) systems was used to identify the optimal coating-process-system combinations. Three coatings were identified as suitable for further study; two CrC NiCr materials and one Fe Ni Cr alloy. No APS-deposited coatings were suitable for the intended application due to poor substrate adhesion (SA) and very high surface roughness (SR). The DJ2700 deposited coating properties were inferior to the coatings deposited using other HVOF systems and thus a Taguchi L18 five parameter, three-level optimization was used to optimize SA of CRC-1 and FE-1. Significant mean increases in bond strength were achieved (147 ± 30% for FE-1 [58 ± 4 MPa] and 12 ± 1% for CRC-1 [67 ± 5 MPa]). An analysis of variance (ANOVA) indicated that the coating bond strengths were primarily dependent on powder flow rate and propane gas flow rate, and also secondarily dependent on spray distance. The optimal deposition parameters identified were: (CRC-1/FE-1) O_2 264/264 standard liters per minute (SLPM); C_3H_8 62/73 SLPM; air 332/311 SLPM; feed rate 30/28 g/min; and spray distance 150/206 mm.

Keywords alloys, ceramics and refractories, injection mould tooling, metals, semimetals, spray coating techniques

1. Introduction

The work detailed in this article was performed under the U.K. Innovative Manufacturing Research Center (IMRC) initiative, within the Warwick Manufacturing Group IMRC, Warwick University, and formed part of a program of work aimed at developing thermally sprayed coatings for the upgrade of low-volume rapidly machined aluminum tooling to higher volume production: Coatings and Processes for Sustainable Mould and Die Protection, Upgrade And Repair (CASPUR).

The use of aluminum alloy for injection mould tools, especially for the automotive industry, is not new (Ref 1-3) and has been utilized as bridge tooling to support the manufacture of typically up to 10,000 components. There is a particular need in the automotive industry for low-cost and rapid tooling that can satisfy component manufacture for volumes between 10,000 and 100,000 because this would support the introduction of vehicles in new and emerging markets where there is considerable design variation and tooling flexibility is required. Achieving the higher volumes with aluminum tooling is difficult due to tool wear, and thus there is a real need for a harder alternative, without the recourse to high-volume production steel tooling with the associated high costs and extensive lead times.

For the protection of steel tooling, hard chrome plating is the most common process. This is very effective at improving wear resistance, but there are increasing concerns over the environmental and social acceptability of the process. All commercial plating baths use hexavalent chromium (Cr^{VI}), which is both highly toxic to the user and hazardous to the environment (Ref 4). Furthermore, electrodeposited Cr coatings are inherently microcracked (Ref 5), which can result in poor corrosion resistance and spalling. Two further hard-coating techniques of note are plasma vapor deposition (Ref 6) and thermal diffusion (Ref 7-9); both of which are used to deposit nitrides (particularly TiN, CrN, and NbN) onto tools (Ref 10, 11) but are severely limited by the size of the application cell. A well-established hard chrome replacement for mechanical components in the automotive and aerospace industry is the high-velocity oxyfuel (HVOF) deposition of tungsten carbide, cobalt (WC-Co) cermet coatings (Ref 12, 13), but the application of this process (and other thermal spray processes) to tooling (Ref 14, 15) has been limited.

The protection of aluminum tooling is somewhat different from the traditional hard chrome plating of moulds, because the substrate material is aluminum (albeit tooling grade) and not tool steel, and thus has significantly different mechanical properties; thus, the performance advantages delivered thermally sprayed coatings were of interest to the author.

In a previous article by the author (Ref 16), the selection, deposition, and evaluation of a wide range of coatings, covering monolithic and particulate composite materials (e.g., WC-Co) (Ref 17), pseudo-alloys (WC or Cr_3C_2 with Ni-, Fe-, or Co-base alloy) (Ref 18), cermets (e.g., Al_2O_3 30 [Ni-20Al]) (Ref 18), pure ceramics (e.g., alumina, zirconia, and chromium oxide) (Ref 19), and also materials of lower hardness (e.g., 316 stainless steel was presented). From the previous evaluation, 10 coatings of specific interest were identified, covering a range of hardness values: tungsten carbide cobalt chrome (WC-10Co-4Cr); chro-

Gregory John Gibbons and **Robert George Hansell,** Warwick Manufacturing Group, School of Engineering, University of Warwick, Coventry, CV4 7AL, U.K. Contact e-mail: g.j.gibbons@warwick.ac.uk.

Table 1 Ranking levels for each down-selection parameter and their associated point-score value

Parameter	Weighting		Scoring				
Substrate adhesions (SA)	3	Level, MPa	<40	40+ to 50	50+ to 60	60+ to 70	>70
		Point score	1	2	3	4	5
Coating quality (CQ)	2	Level	1 to 2.5	2.5+ to 4	4+ to 5.5	5.5+ to 7	7.5+ to 9
		Point score	1	2	3	4	5
Surface roughness (SR)	1	Level, μm	>7	6+ to 7	5+ to 6	4+ to 5	0–4
		Point score	1	2	3	4	5

mium carbide nickel chrome [Cr_2C_3 20 (Ni-20Cr)]; 316 stainless steel (Fe-17Cr-12Ni-2.5Mo-1Si); or alumina-titania mix (Al_2O_3-40TiO_2). These were deposited using HVOF (WC Co Cr, CrC-NiCr, stainless steel) and atmospheric plasma spray (APS) (Al_2O_3-TiO_2). For each of the HVOF and APS system variants, the powder feedstock was selected to have the most suitable particle size, and where possible, the processing route and morphology of the feedstock were maintained consistently throughout each class of materials.

To enable coatings to be evaluated in moulding trials, a further down-selection of the coatings was required because the resources available for the injection moulding trials were sufficient to evaluate two materials only. Furthermore, to ensure that the most strongly adhered coatings were assessed under injection-moulding conditions, the deposition parameters for the two selected coatings were optimized using a robust experimental design. Finally, because the aim of the project was to obtain a commercially capable material-process solution, the process capability of the optimized deposition of each of the two materials was evaluated. The down-selection process used, the results obtained, the subsequent optimization process used, and an analysis of the process capabilities form the content of this article.

2. Experimental Method

2.1 Down-Selection

A matrix was developed from the properties determined in the previous study (Ref 16). The properties were ranked with respect to their perceived order of significance to the application as hard coatings for aluminum tooling. A weighting factor was applied to each of the parameters to quantify the level of perceived importance as judged by the author and through discussion with program partners within the tool-making, injection-moulding, and automotive industries. For each of the parameters, a scale was determined that would encompass the range of measured values for all of the coatings. Each level was designated by a point score. The order of the parameters, their weighting, the scales used, and the point score assigned to each level is given Table 1. Coating adhesion was measured in the prior study using the tensile adhesion-testing method of adhesively bonded loading pins as specified in ASTM C633 (Ref 20). Surface roughness was measured using a Wyko NT-2000 Optical Profiler (Veeco Instruments Ltd, Cambridge, UK), and coating quality (CQ) was assessed through the oxide and porosity area-percentage levels in cross-sectional micrographs, determined using Image C image analysis software (Imtronic, Berlin, Germany).

2.2 Coating Optimization

2.2.1 Sample Preparation for Optimization. Based on the results of the metric analysis down-selection process (see section 3.1), two coatings were chosen for optimization. The adhesion of the coatings to the substrate was chosen as the optimization parameter because the success of the coatings in this application will depend heavily on their ability to maintain adhesion to the substrate while enduring cyclic loadings through both hot polymer injection (at up to 200 MPa) and through component ejection. The CQ was also observed so as to identify any correlation that may occur between CQ (and thus structure) and changes in bond-strength achieved through optimization.

A design-of-experiment approach was used for the optimization. The coatings chosen from the down-selection process were deposited using the HVOF thermal spray process. For a particular hardware configuration, the process is characterized by six continuous experimental factors, three describing the gas flow rates (oxygen, propane, and air), one describing the powder feed rate, one setting the distance between the substrate and the end of the HVOF spray gun (i.e., the standoff distance), and one setting the gun traverse rate. The latter was maintained at a constant 100 mm/s due to limitations of the spray booth hardware. Four of the variable parameters were chosen as three-level factors (three gas flow rates and standoff distance), and, due to the limited system control over powder feed rate, this was chosen as a two-level factor so as to provide sufficient discrimination between the two levels. The Taguchi L18 three level design was used for the optimization (which allows for four three-level factors and one two-level factor). The levels used for the gas and powder flow factors were chosen based on the capability limits of the HVOF system (DJ2600; Sulzer Metco*, Westbury, NY), and the standoff distance levels were chosen based on extrapolation, within sensible limits, of the best practice standoff values for the HVOF deposition of materials. An experimental design sheet was developed from the Taguchi L18 array and is given in Table 2. The process gas pressures were maintained at a constant level throughout the experiment (O_2 1.03 MPa; C_3H_8 0.55 MPa; air 0.52 MPa; and N_2 powder feed carrier gas 1.03 MPa). N_2 pressure was not used as an experimental factor because the level for this parameter is specified by the manufacturer and is required for correct operation of the powder feed system.

2.2.2 Tensile Adhesion Testing. Each of the down-selected coatings was deposited onto grit-blast prepared aluminum (2014; Alcoa Europe, Birmingham, UK) substrates using each of the 18 process parameter sets of Table 1 to a thickness of 100 μm. The coated substrates were cut into 25 × 25 mm squares to create substrate fixtures. Tensile adhesion testing was performed using the method prescribed in ASTM C633-01 (Ref

Table 2 Design sheet employed for the coating deposition optimization

Experiment No.	Factor				
	Feed rate, g/min	Oxygen, SLPM	Propane, SLPM	Air, SLPM	Distance, mm
1	15	219	66	311	150
2	15	219	75	346	225
3	15	219	82	381	300
4	15	242	66	311	225
5	15	242	75	346	300
6	15	242	82	381	150
7	15	264	66	346	150
8	15	264	75	381	225
9	15	264	82	311	300
10	30	219	66	381	300
11	30	219	75	311	150
12	30	219	82	346	225
13	30	242	66	346	300
14	30	242	75	381	150
15	30	242	82	311	225
16	30	264	66	381	225
17	30	264	75	311	300
18	30	264	82	346	150

SLPM, standard liters per minute

20). The loading fixture was alumina grit-blasted at 0.3 MPa (Vixograin 125-177 μm media; Vixen Surface Treatments Ltd, Stockton-on-Tees, UK). The two fixtures were bonded together using FM1000 (Cytec Engineered Materials Ltd., Wrexham, UK) polyamide-epoxy unsupported adhesive film, grade 0.15 ± 0.025 kg/m^3. This adhesive was chosen because it has minimal flow at elevated temperature, which was desirable for preventing the potential ingress of the adhesive through coating and bonding at the coating-substrate interface. The adhesive was cured in air at 175 °C for 1 h. Proper measures were taken to maintain normal alignment between the fixtures and consistent pressure on the bond line during curing. Tensile testing was performed on an Instron 4505 (Instron, High Wycombe, UK) with a 100 kN load cell. A grip distance of 20 ± 1 mm was used with a cross-head speed of 2 mm/min and testing was performed at 23 ± 1 °C and 55 ± 2% Rh. Five samples of each coating were prepared and evaluated.

2.2.3 Microstructural Analysis. Samples of the coated substrates were prepared metallurgically by mounting with a cold set epoxy resin (Triofix 2; Struers Ltd., Glasgow, UK), grinding with silicon carbide papers down to 1200 grit, and polishing down to 1 μm using diamond paste, and were final polished using colloidal silica for 1 min. The coating microstructure was imaged using an Optophot microscope (Nikon, Tokyo, Japan) at between 100× and 400× magnification, and the images were recorded using a Camedia C-3030 digital camera (Olympus, Tokyo, Japan).

2.2.4 Sample Preparation and Evaluation for Confirmation. To confirm the optimization results, a confirmation experiment was performed. Samples were deposited to 100 μm using the optimum values obtained from the analysis for the O_2, C_3H_8, and air gas flow rates, the powder flow rate, and the standoff distance. The constant parameter levels were maintained as for the original sample preparation (section 2.2.1). Again, the coated substrates were cut into 30 × 30 mm squares for analysis. The SR (Ra) was measured using a Wyko NT-2000 Optical Profiler (Vecco Instruments Inc., Woodbury, NY), the SA was measured as described in section 2.2.2, and the CQ was measured using the method described in section 2.2.3 and employed Image C image analysis software to determine the area percentage of porosity of the coating cross section.

3. Experimental Results

3.1 Down-Selection Metric Evaluation

The matrix of Table 1 was applied to the results of the coating evaluation described previously (Ref 16) to obtain a ranked overall point score value (PSV) for each coating. The values obtained were used for coating down-selection, and the results of this process are given in Table 3. The coatings are identified by "CRC" [Cr_2C_3-20(20NiCr)], "WC" (WC-10Co-4Cr), "FE" (Fe-17Cr-12Ni-2.5Mo-1Si), or "AT" (Al_2O_3-40TiO_2).

3.2 Coating Optimization

The results of the optimization experiments for CRC-1 and FE-1 (Ni-20Cr-10W-9Mo-4Cu-1C-1B-1Fe) were analyzed using commercially available statistical software (DOE Pro XL; Digital Computations Inc, Colorado Springs, CO). An analysis of variance (ANOVA) of each of the data sets was performed; the results of this are given in Table 4.

A least-squares regression was performed on each of the data sets, which was repeated after removing all insignificant factors from the regression [P > 0.4 (two-tailed)]. The performance of each system was then optimized. For the optimization, all factors were treated as continuous, and a Y-hat model with a constraint to achieve maximum bond strength was used. The results of the response prediction and the associated optimal experimental parameters required to achieve the predicted response are given in Table 5. The parameters used in the prior work (Ref 16), and used to prepare samples for down-selection, are also presented in Table 5 for comparison. The relationship between the two most significant parameters for each coating and the predicted response (bond strength) is given in Fig. 1 (CRC-1) and Fig. 2 (FE-1). In each case, all other experimental parameters were set at the optimal values, as given in Table 5 and section 2.2.1.

The results of the confirmation experiment are given in Table 6, which contains the SA, and the SA, SR, CQ, and total PSVs for the nonoptimized and optimized CRC-1 and FE-1 coatings. The microstructure of CRC-1 and FE-1 deposited using the optimal parameters are shown in Fig. 3 and 4, respectively, which compare these coating microstructures to their equivalent nonoptimized coating microstructures. The nonoptimized micrographs represent the structure of the poorest quality coating obtained for each of the 18 Taguchi experiments, and were deposited using the parameters of experiment 13 (Table 2). A process capability analysis of the confirmation data for each coating was performed, the results of which are given in Table 7

4. Discussion

4.1 Coating Down-Selection

From Table 3, it is clear that the APS systems provide very poor levels of SA to the Al_2O_3-TiO_2 coatings (as seen from the low SA PSV). This is highly detrimental to their performance as

Table 3 Point score value results for each of the coatings identified in the previous work

		WC 10Co 4Cr PSV				Material Cr_2C_3 25(Ni20Cr) PSV					Fe17Cr12Ni2.5Mo1Si PSV					Al_2O_3-40TiO_2 PSV				
System	Name	SA	SR	CQ	Total	Name	SA	SR	CQ	Total	Name	SA	SR	CQ	Total	Name	SA	SR	CQ	Total
HVOF																				
DJ 2700	WC-1	9	1	2	12	CRC-1	9	4	6	19	FE-1	3	1	6	10	…	…	…	…	…
JP5000	WC-2	15	5	10	30	CRC-2	15	4	10	29	FE-2	12	1	10	23					
Jet Kote IIa	WC-3	15	4	10	29	CRC-3	15	2	10	27	…	…	…	…	…	…	…	…	…	…
APS																				
9M	…	…	…	…	…	…	…	…	…	…	…	…	…	…	…	AT-1	3	1	2	6
PT-F4	…	…	…	…	…	…	…	…	…	…	…	…	…	…	…	AT-2	3	1	10	14

Table 4 Analysis of variance statistical results for initial L18 Taguchi experiment

		CRC-1		FE-1	
Source	df	*F*	% Contribution	*F*	% Contribution
Feed rate	1	2.085	16.35	0.049	0.22
Oxygen	2	0.274	4.30	1.033	9.43
Propane	2	0.282	4.42	2.644	24.14
Air	2	0.163	2.56	1.073	9.80
Distance	2	0.867	13.59	1.983	18.11
Average bond	2	0.748	11.73	1.194	10.90
Error	6	2.085	47.04	…	27.39

df, degree of freedom

injection mould tool coatings because this would provide a likely means for early coating failure under moulding conditions. Furthermore, the coatings suffer from high SR values (low SR PSV). Although SR is not weighted highly (Table 1), this would limit their application to the production of mouldings where surface finish is less important (e.g., under bonnet automotive applications) because it would be very difficult to achieve a smooth finish for the extremely hard Al_2O_3-TiO_2. AT-1 and AT-2 were thus eliminated from further down-selection.

The WC coating that performed the best was WC-2, which was deposited using the JP5000 HVOF system (Praxair Tafa Inc, Indianapolis, IN), which achieved a maximum PSV of 30 (Table 3). This was closely matched by the Jet Kote IIa (Deloro Stellite, Swindon, UK) deposited coating, WC-3, which suffered from a slightly rougher as-sprayed finish. The coating that performed the poorest was WC-1 (DJ2700; Sulzer Metco (UK) Ltd., Risca, UK), having a high SR and poor CQ, although the SA was reasonable (PSV 3).

There is less differentiation between the performance of the CRC coatings (Table 3), although again, the JP5000 and Jet Kote IIa coatings (CRC-2 and CRC-3, respectively) outperform the DJ2700-deposited coating (CRC-1), particularly in the SA and CQ performance indicators. It is noted though that Jet-Kote IIa-deposited CRC-3 is a significantly rougher coating than both CRC-1 and CRC-2, although this does not detract significantly from the overall PSV for CRC-3. Again though, as for the APS-deposited coatings, the high SR and high hardness limit this coating to moulding components where aesthetics are not important.

It is very clear from Table 3 that the DJ2700 HVOF deposition of FE-1 offers a very poor performance coating, with very low SA (SA 3) and high SR (SR1). In contrast to this, the JP5000-deposited FE-2 displays very good SA (SA 12), although SR was still high (SR1). Both coatings displayed an average microstructure (CQ 6).

The down-selection results clearly indicate that WC-2 and CRC-2, both deposited using the JP5000 HVOF system, have the most suitable properties and, indeed, have potential for the development of a commercial process for this application. Within the CASPUR project, it was identified that for further investigation, especially mould tool evaluation, the authors required control over HVOF deposition parameters, which could only be realized entirely by using the DJ 2700 HVOF system. It was thus decided that the optimization process would be focused on the DJ2700 HVOF deposition of CRC-1 and FE-1. Both of these coatings suffered from low surface adhesion values (Table 3), and it was this response that was the focus of the optimization. Also, the coating qualities of CRC-1 and FE-1 was lower than for their counterparts CRC-2, CRC-3, and FE-2, and the effect of SA optimization on this was also evaluated during the optimization process.

4.2 Coating Optimization

From the results of the ANOVA analysis (Table 4), it is observed that the most significant factor affecting the response (bond strength) is different for each coating, being "feed rate" for CRC-1 (16.35%) and "propane feed rate" for FE-1 (24.14%). For both coatings, the response is sensitive to the spray distance, with contributions of 13.59 and 18.11%, respectively, for CRC-1 and FE-1, and is the second most significant factor for both materials. Because there was little change in the setting of the spray distance between the initial and optimized values for both CRC-1 and FE-1 (0% and +3%, respectively), this parameter can be assumed to have had little effect on the improvements observed in the optimized coating properties.

The relationship between the two principal control parameters for each of the materials is quite dissimilar. For CRC-1, the relationship is linear (Fig. 1), with only one solution for optimum response (55–60 MPa), processing at minimum spray distance and maximum powder feed rate. For FE-1, the relationship is more complex, with the surface plot having a saddle structure (Fig. 2). The best response (60-66 MPa region) is obtained for high propane flow rates and a spray distance median between the upper and lower experimental limits. The response is lower for both lower and higher spray distances for all propane flow rates. For higher spray distances, this may be expected as the upper spray distance will result in lower velocity and cooler particles hitting the substrate.

The reduction in bond strength for shorter spray distances is in conflict with the optimum distance observed for CRC-1, but

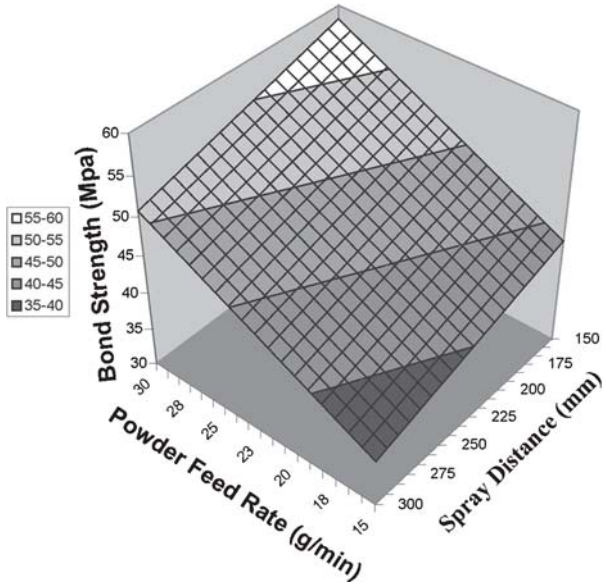

Fig. 1 Bond strength response to the variation in spray distance and powder feed rate for CRC-1

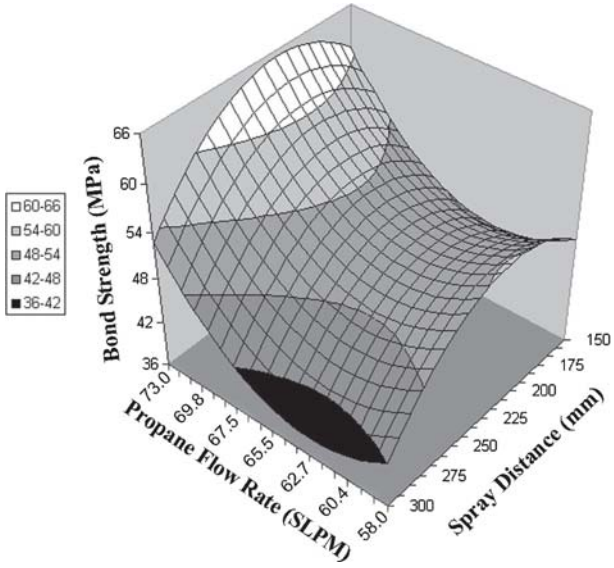

Fig. 2 Bond strength response to the variation in propane flow rate and spray distance for FE-1

Table 5 Results of the optimized regression for the DJ 2700 high-velocity oxyfuel deposition of CRC-1 and FE-1

		Prediction 99% Confidence interval		Previous/optimal experimental parameters				
Coating	Y-hat	Lower bound	Upper bound	Feed rate, g/min	Oxygen, SLPM	Propane, SLPM	Air, SLPM	Distance, mm
CRC-1	56 ± 8	32	80	23/30(a)	281/264	66/62	329/332	150/150(a)
	…	…	…	**(+30%)**	(−6%)	(−6%)	(+0.9%)	(0% change)
FE-1	65 ± 10	35	95	28/30	263/264	63/73(a)	378/311	200/206(a)
	…	…	…	(+7%)	(+0.4%)	**(+16%)**	**(−18%)**	(+3%)

(a) Indicates most significant factors as identified from ANOVA analysis (Fig. 4). Bold numbers represent largest changes between nonoptimized and optimized bond-strengths.

this may result from excessive thermal energy transfer into the substrate, which, as a result of the differential expansion between the substrate and coating on cooling, compromises the coating-substrate bond. Furthermore, excessive heating of the substrate may further oxidize the substrate, reducing the adhesion of the coating, as is suggested by Gil and Staia (Ref 21) for the HVOF deposition of NiWCrBSi alloy onto an AISI 1020 steel substrate.

A further insight into the causes of the strong dependence of the quality of FE-1 on the propane feed rate is given by examining the equivalence ratio F for the gas feed rates [as used by Gill and Staia (Ref 21)], where F is the ratio $[(F/O)_{actual}/(F/O)_{stoich}]$, where $(F/O)_{actual}$ is the mass ratio of fuel to oxygen actually used, and $(F/O)_{stoich}$ is the mass ratio of fuel to oxygen under stoichiometric conditions (which for the propane-air combustion reaction is 0.2).

By considering the gas flow rates used in the nonoptimized and optimized deposition of FE-1, it is seen that there is a move from oxidative flame condition ($F = 1.1$) for the nonoptimized deposition to a reducing condition ($F = 0.9$) for the optimized deposition. It has been previously indicated that the maximum flame temperature is achieved for slightly reducing conditions (Ref 21) because a lean flame will not be cooled by the presence of unburned oxygen. The higher flame temperature under these conditions may ensure fuller melting of the particles, and thus the development of laminar splats during impact, resulting in higher mechanical interlocking forces between the particles and substrate (Ref 22). Furthermore, the protection against particle oxidation offered by the reducing flame may encourage a more homogeneous microstructure to develop, which again contributes to the observed improvement in adhesion (Ref 21).

Interestingly, the bond strength response increases slightly for lower propane flow rates, and indeed rises into the 54 to 60 MPa response region at a propane flow rate of 58.0 standard liters per minute (SLPM). The response of the system at propane flow rates below 58.0 SLPM is not known, and is not measurable because it is not possible to operate the DJ2700 system at lower propane gas flow rates (when using the optimal O_2 and airflow rates). Thus, to obtain optimally bound coatings, the upper propane gas flow rate (~73.0 SLPM) must be used. The reasons for this slight increase at lower propane flow rates is unknown, and further investigation will be required to describe this phenomenon.

Both the optimized and nonoptimized CRC-1 coatings were deposited under oxidizing flame conditions ($F = 0.9$) and nearly identical total gas flow rates, which implies that the temperature and velocity of the flame would be very similar in both cases (Ref 21, 23, 24). Because the spray distance is constant for each

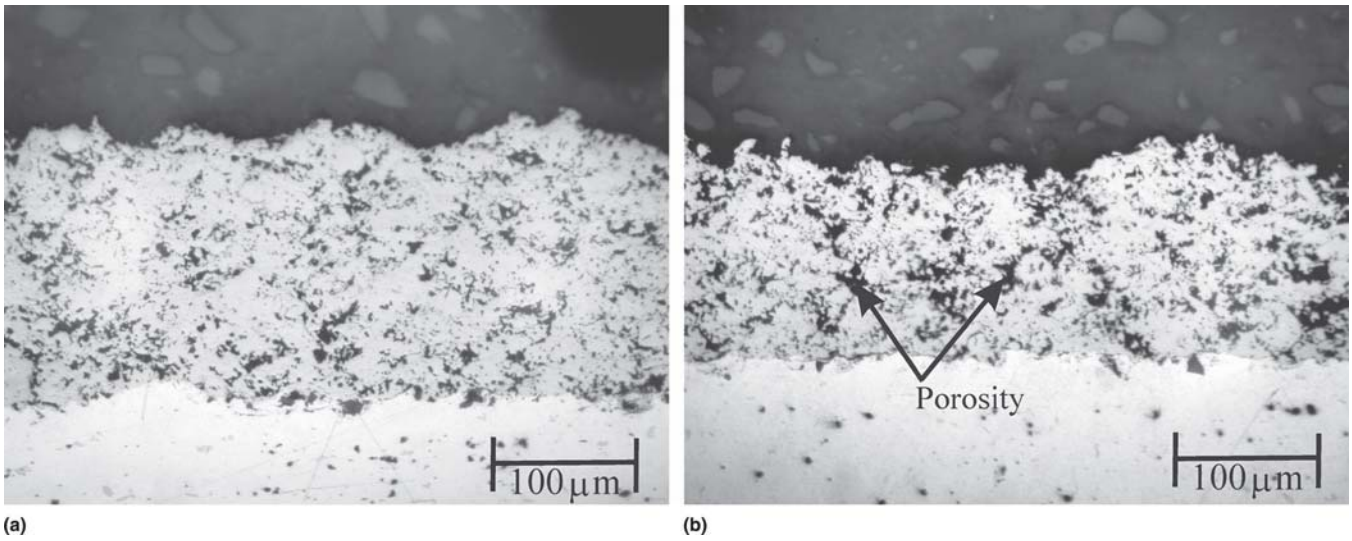

Fig. 3 Microstructure of optimized (a) and nonoptimized (b) CRC-1 (Cr_2C_3) 20(20NiCr) coatings

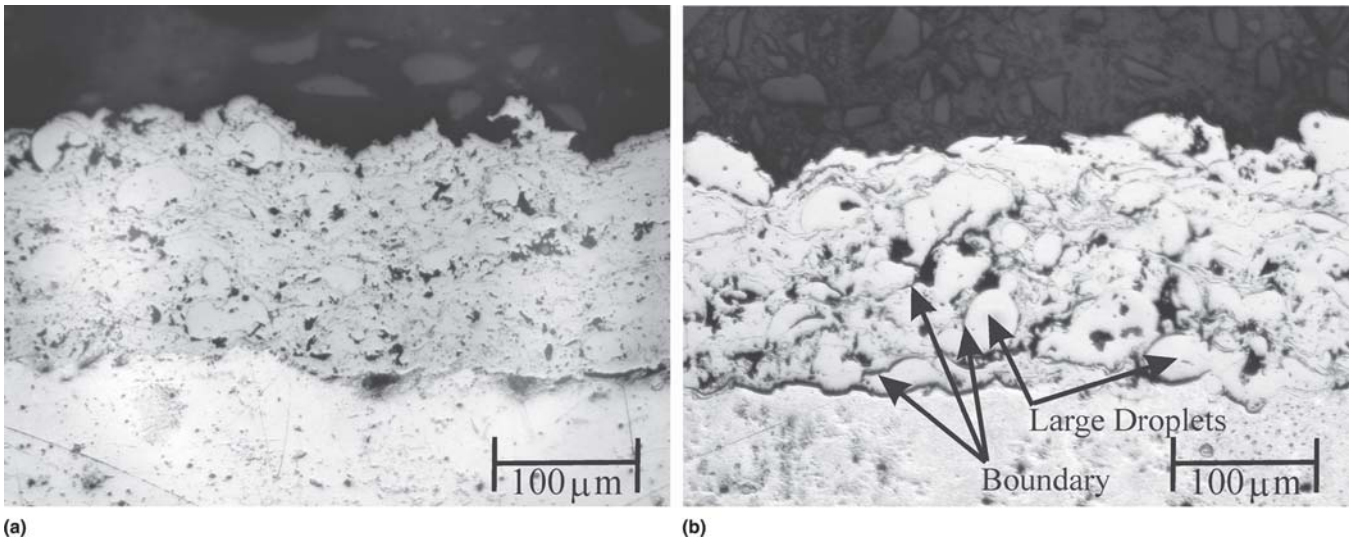

Fig. 4 Microstructure of optimized (a) and nonoptimized (b) FE-1 (Ni-20Cr-10W-9Mo-4Cu-1C-1B-1Fe) coatings

Table 6 Results of the confirmation experiment

Sample	Average bond strength, nonoptimized, MPa	Average bond strength, optimized, MPa	Point score value (PSV)							
			Nonoptimized				Optimized			
			SA	SR	CQ	Total	SA	SR	CQ	Total
CRC-1	23.6 ± 0.9	58 ± 4	9	4	6	19	12	4	8	24
FE-1	60 ± 3	67 ± 5	3	1	6	10	12	1	8	21

case, it is inferred that the observed improvement in adhesion resulting from the optimization is due to the increase in feed rate. It is known that the overheating of CrC-NiCr can result in decomposition of the carbides (Ref 25), and, indeed, an increase in the powder feed rate in the HVOF deposition of the alloy has been observed to decrease the particle temperature (Ref 24). This reduction would reduce carbide dissolution in the NiCr matrix and thus provide a larger residual number of hard particles that could provide a peening effect on the coating, which is mooted as being important in providing a compressive stress in the coating, and thus improving adhesion (Ref 22).

The results of the confirmation experiment (Table 6) clearly demonstrate the benefit of optimization and also confirm the Y-hat prediction obtained from the linear regression (Table 5). The changes in HVOF operating parameters that occurred as a result of the optimization (as indicated in Table 5) are in agreement with the process sensitivities identified through the ANOVA analysis (Table 4). The average adhesive bond strengths for

Table 7 Process capability analysis for optimized deposition of CRC-1 and FE-1

	USL-LSL 200–60 MPa		USL-LSL 200–50 MPa		USL-LSL 200–40 MPa		USL-LSL 200–30 MPa	
Coating	DPM	Cpk	DPM	Cpk	DPM	Cpk	DPM	Cpk
CRC-1	559,731	−0.05	214,192	0.26	41,441	0.58	3,720	0.89
FE-1	247,749	0.23	45,265	0.56	3,430	0.90	102	1.24

USL, upper spec limit; LSL, lower spec limit; DPM, defects per million; Cpk, process capability index

CRC-1 and FE-1 were increased from the mean nonoptimized values of 60 ± 3 MPa and 23.6 ± 0.9 MPa, respectively, to 67 ± 5 MPa and 58 ± 4 MPa, respectively (a mean increase of 12 ± 1% and 147 ± 30%, respectively), and each optimized value was within the range predicted by the Y-hat regression (Table 5). For coatings optimized for the highest bond strength, the quality of the microstructure obtained was also improved (Fig. 3, 4). The improvement in coating microstructure quality for CRC-1 was primarily characterized by a significant decrease in porosity (indicated by the black regions of Fig. 3). The nonoptimized microstructure of FE-1 was observed to contain a large number of droplets of large size, with porosity between them (Fig. 4). The quality was improved on optimization by a reduction in the droplet size, the elimination of the boundary between them, and the creation of a more homogeneous structure.

Although the optimization offered some reduction in porosity levels for both FE-1 and CRC-1 (potentially achieved through oxidation protection as discussed above) (Ref 21), there were still significant levels of porosity remaining in the coatings. It is known, though, that for other alloy coatings (e.g., NiWCrBSi) the spray distance has a very significant effect on porosity levels, and, thus, the further optimization of porosity is likely to be required to achieve a better CQ (although the processing requirements for porosity and adhesion may be in conflict with each other, because too short a spray distance has been suggested as being detrimental to the adhesion of coatings) (Ref 21).

No improvement in SR was observed for either coating (Table 6). It may be possible to deliver an improvement through optimization, although this is not considered justified due to the low importance attached to SR (a weighting of 1 in Table 1).

The total PSV of 24 for optimized CRC-1 (Table 6) brings an overall quality that is similar to those of CRC-2 and CRC-3. Indeed, within the upper error band of the measured SA, the SA PSV for CRC-2 is within the 60 + MPa region of Table 1 and thus would provide the coating with a total PSV of 27, equaling that of CRC-3. The improvements in coating properties for FE-1, and in particular the substantially increased SA (Table 6), significantly raise the PSV rating for the coating, making it as attractive as the FE-2 coating for this application. Again, as for CRC-1, within the upper error band of the SA, the SA PSV surpasses that of FE-2 and puts each coating on a total PSV of 24. Thus, through optimization of the surface adhesion, it has been possible to develop both a CrC-NiCr and an Fe-17Cr-12Ni coating process using the DJ2700 HVOF system that equals the properties of the Jet-Kote-deposited coating (CRC only) and almost matches those of the JP5000 coatings.

Furthermore, with reference to Table 7, the HVOF deposition of FE-1 is a more capable process than the deposition of CRC-1, as indicated by the lower number of defects for each specification limit and by the higher process capability index for an equivalent specification limit. The process capability index (Cpk) of 1.24 is equivalent to 3.7 Σ, which is below the minimum generally required for an industrial process (4 Σ), and thus further optimization of the process should be used to achieve this level of capability.

5. Conclusions

Two thermal spray materials, one Cr_2C_3 25(Ni-20Cr) and one WC-10Co-4Cr, deposited using JP5000 HVOF hardware, have been shown to offer properties that could enable low-cost, low-volume production aluminum injection mould tooling to be upgraded to higher volume production tooling. Using these coatings, the significant cost advantages provided by rapidly machined aluminum tooling for low-volume manufacture may be extended further into higher-volume manufacture, increasing their flexibility and offering continued time and cost savings to the ordinary equipment manufacturer (OEM).

The properties of coatings deposited using standard parameters with DJ2700 hardware were inferior to the Jet-Kote and JP5000 equivalent coatings for application to injection mould tool coatings. In particular, the SA of both Cr_2C_3 25(Ni20Cr) and WC-10Co-4Cr was significantly lower than their equivalents. Through a Taguchi optimization procedure for the DJ2700 deposition, the SA of both coatings was significantly increased to a level consistent with that obtained through the other HVOF systems. Furthermore, the microstructure of the coatings was also improved. There was no observed improvement in surface finish, although this may be possible through further optimization processes.

The most significant deposition parameter was different for each coating (powder feed rate for CRC-1 and propane gas flow rate for FE-1). The dependence was linear for CRC-1 (maximum response at maximum powder flow rate) and nonlinear for FE-1 (maximum response at both minimum and maximum gas flow rate). The spray distance was found to be a sensitive parameter that is common to both coatings, and again the bond-strength dependence was different for each coating, linear for CRC-1 (maximum response at maximum powder flow rate) and nonlinear for FE-1 (maximum response at intermediate spray distance).

A process-capability analysis of the deposition of CRC-1 and FE-1 using optimal parameters has shown that the deposition of FE-1 is a more capable process (3.7 Σ) than the deposition of CRC-1 (2.7 Σ), and thus the deposition of FE-1 using DJ2700 hardware is the more favorable process for this application.

CRC-1 and FE-1 (DJ2700 deposited) and CRC-3 were subsequently evaluated in tooling trials (the subject of a further article by this author as yet unpublished). The DJ2700 coatings were deposited onto flat plaque inserts using the optimized pa-

rameters obtained from this study. Although these trials were limited, both coatings successfully produced 200 mouldings in 30% glass-filled polyamide, which were injected at 22 MPa and 220 °C. Further trials are underway at the present time on a tool containing geometry that is more representative of an automotive component, and these results will be included in the further article by this author.

Acknowledgment

The author wishes to thank the Engineering and Physical Sciences Research Council for financial support of this research under the Warwick Innovative Manufacturing Research Centre.

References

1. R.T. Evans and G. Zerkowski, Aluminium Alloy for Moulding Tools, *Plast. Rubber Int.,* 1977, **2**(4), p 173-175
2. H. Adickes, Moulds of Aluminium for Processing Plastics Into Motor Car Parts, *Kunstoffe German Plast.,* 1984, **74**(5), p 11-12
3. A. Erstling, Aluminium Insert Application in Injection Mould Tools, *Kunstoffe German Plast.,* 1988, **78**(7), p 16-17
4. K. Hughes, M.E. Meek, L.J. Seed, and J. Shedden, Chromium and its Compounds: Evaluation of Risks to Health from Environment Exposure in Canada: Environmental Carcinogenesis and Ecotoxicology Reviews (Part C), *J. Environ. Sci. Health, Part C,* 1994, **12**(2), p 237-256
5. M. McCormick and S.J. Dobson, Characteristics and Properties of Electrodeposited Chromium from Solutions With Varying Sulphate Ratios, *Technical Papers, Annual Technical Conference and Exhibition, Institute of Metal Finishing,* Vol 2, 1986, p 183-220
6. L.A. Dobrzanski, M. Polok, P. Panjan, S. Bugliosi, and M. Adamiak, Improvement of Wear Resistance of Hot Work Steels By PVD Coatings Deposition, *J. Mater. Proc. Technol.,* 2004, **155-156**(1-3), p 1995–2001
7. H.M. Glaser, Thermal Diffusion (TD) Process Technology And Case Studies, *Adv. Powder Metall.,* 1991, **1,** p 155-166
8. T. Arai and D.L. Hallum, Coating Greatly Expands Tool Life, *Am. Machinist,* 1995, **139**(11), p 37-39
9. S.A. Plumb, C.G. Smith, J.D. Smith, and S. Nitrotec, An Environmentally Friendly Alternative to Hard Chromium Plating, *Trans. Inst. Metal Finish.,* 1999, **77**(1), p B12-B16
10. N. Dingremont, E. Bergmann, and P. Collignon, Application of Duplex Coatings for Metal Injection Moulding, *Surf. Coat. Technol.,* 1995, **72**(3), p 157-162
11. B. Navinsek, P. Panjan, and J. Krusic, Hard Coatings on Soft Metallic Substrates, *Surf. Coat. Technol.,* 1998, **98**(1-3), p 809-815
12. B.D. Sartwell, Thermal Spray Coatings as an Alternative to Hard Chrome Plating, *Weld J.,* 2000, **79**(7), p 39-43
13. L. Valentinelli, T. Valente, F. Casadei, and L. Fedrizzi, Mechanical and Tribocorrosion Properties of HVOF Sprayed WC-Co Coatings, *Corros. Eng. Sci. Technol.,* 2004, **39**(4), p 301-307
14. H. Henke, A. Dietrich, A. Kohler, and R.B. Heimann, Development and Testing of HVOF-Sprayed Tungsten Carbide Coatings Applied to Moulds for Concrete Roof Tiles, *Wear,* 2004, **256**(1-2), p 81-87
15. C. Li, M. Kato, K. Nakasa, and D. Zhang, Effect of Cyclic Surface Pressure on Delamination Strength of WC-Co Coating Sprayed by HP-HVOF, *J. Soc. Mater. Sci.,* 2002, **51**(8), p 892-899, in Japanese
16. G.J. Gibbons and R.G. Hansell, Thermal-Sprayed Coatings on Aluminium for Mould Tool Protection and Upgrade, *J. Mater. Proc. Technol.,* in press
17. R.W. Smith and R. Novak, Advances and Applications in U.S. Thermal Spray Technology I: Technology and Materials, *Powder Metall. Int.,* 1991, **23**(3), p 147-155
18. E. Lugscheider, H. Eschnauer, U. Mueller, and Th. Weber, Quo Vadis, Thermal Spray Technology, *Powder Metall. Int.,* 1991, **23**(1), p 33-39
19. J.C. Bailey, Metal Spraying, *Engineering (London),* 1979, **219**(9), p i-viii
20. "Standard Test Method for Adhesion or Cohesion Strength of Thermal Spray Coatings" C633-01, *Annual Book of Standards,* Vol 02.05, ASM International, 2005
21. L.E. Gil and M.H. Staia, Effects of HVOF parameters on Adhesion and Microstructure of Thermal Sprayed NiWCrBSi Coatings, *Surf. Eng.,* 2002, **18**(4), p 309-315
22. C.J. Li and Y.Y. Wang, Effect of Particle State on the Adhesive Strength of HVOF Sprayed Metallic Coating, *J. Therm. Spray Technol.,* 2002, **11**(4), p 523-529
23. L. Zhao, M. Maurer, F. Fischer, and E. Lugscheider, Study of HVOF Spraying o WC-CoCr Using On-Line Particle Monitoring, *Surf. Coat. Technol.,* 2004, **185,** p 160-165
24. L. Zhao, M. Maurer, F. Fischer, R. Dicks, and E. Lugscheider, Influence of Spray Parameters on the In-Flight Properties and the Properties of HVOF Coating of WC-CoCr, *Wear,* 2004, **257,** p 41-46
25. C.J. Li, K. Sonoya, G.C. Ji, and Y.Y. Wang, Effect of Soray Conditions on the Properties of HVOF Cr_3C_2-NiCr Coatings, *Weld. World,* 1998, **41,** p 77-87